BASIC SCIENCE

Nanomedicine: Nanotechnology, Biology, and Medicine 6 (2010) 808–814

nanomedicine

www.nanomedjournal.com

Original Article

Effect of cholesterol and amyloid-β peptide on structure and function of mixed-lipid films and pulmonary surfactant BLES: an atomic force microscopy study

Francis Hane, MSc, BSc[a], Elizabeth Drolle, BSc[a], Zoya Leonenko, BSc, PhD[a,b,*]

[a]*Department of Biology, University of Waterloo, Waterloo, Canada*

[b]*Department of Physics and Astronomy, University of Waterloo, Waterloo, Canada*

Received 3 February 2010; accepted 3 May 2010

Abstract

Pulmonary surfactant forms a thin molecular film inside mammalian lung alveoli and lowers the surface tension of the air/fluid interface to reduce the work of breathing. Upon compression functional surfactant forms characteristic multilayer structures, which indicate surfactant surface activity. We showed that cholesterol adversely affects both structural and surface-active properties of BLES surfactant and DPPC/DOPG lipid films. Incorporation of small concentrations of fibril-forming peptide amyloid-β 1-40 helps to counteract the distractive effect of cholesterol by improving characteristic multilayer formation that occurs upon compression. In contrast to many negative effects of amyloid-forming peptides reported earlier, we report a positive effect of amyloid-β peptide on surfactant function, which may aid in the designing of novel surfactant formulations.

From the Clinical Editor: The authors demonstrate the adverse effects of cholesterol from the standpoint of the structural and surface active properties of lipid films and surfactants. Incorporation of small concentrations of fibril forming peptide amyloid-ß 1-40 helps to counteract the effects of cholesterol, in contrast to many negative effects of amyloid forming peptides reported earlier.

Key words: Lipid; Protein; Pulmonary surfactant; Surfactant dysfunction; Cholesterol; Amyloid-β; Nanoscale structure; Atomic force microscopy

Pulmonary surfactant (PS) is a complex lipid-protein mixture that forms a monomolecular film at the air/lung interface.[1] The function of PS film is to reduce the surface tension of the alveolar air/liquid interface, thus reducing the work of breathing.[2-4] The PS film primarily consists of phospholipids: phosphatidylcholine (PC) composes 70 to 80% of the surfactant mixture, with 50 to 70% of the PC being saturated lipids.[5,6] The other 10% of the mixture are surfactant-specific proteins (A, B, C, and D).[5,6] A small amount of cholesterol is also present at 5 to 10%. In order for PS to be functional and maintain its interfacial properties, the balance of PS film composition is necessary to allow the surfactant surface tension to be reduced to very low values, which approach 0 mN/m, as well as to allow PS film to respread rapidly during the respiratory cycle. The primary lipid, dipalmitoylphosphatidylcholine (DPPC), is capable of reducing surface tensions to values approaching zero, but DPPC alone is inadequate as an effective surfactant and is slow to respread when compression is relieved, and is slow to absorb from an aqueous suspension.[7] Previously, we and others[8,9] have shown that the characteristic feature of functional surfactant, which correlates with its surface-active properties, is its ability to form multilayer structures upon compression. We have also shown that performance of the pulmonary surfactant bovine lung extract surfactant (BLES)[8,10] is strongly affected by excess cholesterol (20%), and in this work we show that model lipid films are as well. The excess cholesterol impairs characteristic multilayer formation and ability of the film to reduce the surface tension to near zero values.[8]

One of the important components in the surfactant mixture, aiding in the enhancement of surface-active properties, is surfactant-specific protein C (SP-C), a hydrophobic α-helical transmembrane protein.[11] SP-C contains two palmitoyl groups covalently bound to Cys-5 and Cys-6 and plays an important role in assisting the multilayer formation when the film is compressed.[8,12] The α-helical region becomes embedded in the bilayer, as the length of the α-helix matches the thickness of bilayer, and two palmitoyl groups become embedded into the lipid monolayer serving as an anchor, linking the multilayers and monolayer.[8,9,13] The α-helical region acts also as a hinge assisting

Funding sources: Natural Sciences and Engineering Council of Canada (NSERC), Canada Foundation for Innovation (CFI), Ontario Ministry of Research and Innovation, Ontario Research Fund (ORF) and NSERC Undergraduate Student Research Award to ED.

*Corresponding author: University of Waterloo, 200 University Avenue, Waterloo, Ontario, Canada N2L 3G1.

E-mail address: zleonenk@scimail.uwaterloo.ca (Z. Leonenko).

1549-9634/$ – see front matter © 2010 Elsevier Inc. All rights reserved.
doi:10.1016/j.nano.2010.05.001

in bilayer formation.[8,13] This mechanism is discussed in our previous publication.[8] SP-C has been shown to misfold and form amyloid-type fibrils,[14,15] which is common for more than 20 other fibril-forming proteins. Fibrillogenesis is associated with various neurodegenerative diseases, such as Alzheimer's or Parkinson's diseases.[16-20] In pulmonary surfactant the fibrillization is associated with pulmonary alveolar proteinosis.[15] SP-C forms amyloid fibrils similar to the fibrils formed by amyloid-β protein, implicated in Alzheimer's disease.[17,18] Both SP-C and amyloid-β peptide contain α-helical regions, which can be incorporated into the lipid membrane. Considering that amyloid-β has two α-helical regions connected by a small random coil section, we postulated that amyloid-β may act as a molecular hinge joining lipid mono-and bilayers, and assist in respreading of surfactant, similar to SP-C. In this work we investigated the effect of amyloid-β on the surface activity of BLES surfactant and model mixed-lipid films (DPPC-DOPG) with and without cholesterol. Using atomic force microscopy (AFM) and the Langmuir-Blodgett monolayer technique, we showed that amyloid-β helps to counteract the distractive effect of cholesterol by improving structural morphology of the films (multilayer formation), which is almost completely inhibited by excess cholesterol. This study may aid in the understanding of the effect of amyloid-forming peptides on structure and function of lung surfactant BLES and mixed-lipid films, which can be considered as a simple artificial surfactant. Understanding the molecular mechanism of PS function as well as simpler synthetic lipid mixtures provides an important basis for successful development of synthetic surfactant formulations, which are required for treatment of the respiratory diseases (such as respiratory distress syndrome [RDS] or neonatal respiratory distress syndrome [NRDS]).[21] Currently exogenous surfactant formulations extracted from bovine or porcine lungs are commonly administered to treat patients with lack of surfactant or surfactant failure. For example, BLES (BLES Biochemicals, London, Ontario, Canada), Curosurf (Chiesi Pharmaceutici, Parma, Italy), Survanta (Ross Laboratories Columbus, Ohio), and Surfacten (Surfactant TA; Mitsubishi Pharma Corporation, Tokyo, Japan) are analogues to native pulmonary surfactant, and are clinically used in each country. Although animal extracts are effective in treating patients, they are associated with a costly purification procedure to eliminate the risks of infections, and also with the difficulties of producing batch-to-batch uniformity. Therefore, preparations of pure synthetic surfactants are highly desired in the clinical surfactant replacement therapy. Simple multicomponent lipid mixtures were tested as synthetic surfactant formulations,[22-25] as well as lipid mixtures with addition of synthetic helical peptides.[9,24,26,27] In this work we explored the effect of incorporation of amyloid-β peptide into DPPC-DOPG mixture on the structure and function of BLES and artificial lipid mixtures, which may also aid in designing noble artificial surfactant formulations.

Methods

Sample preparation

1,2-Dipalmitoyl-sn-glycero-3-phosphocholine (DPPC) and 1,2-dioleoyl-sn-glycero-3-phospho-(1′-rac-glycerol) (DOPG) (Avanti Polar Lipids, Inc., Alabaster, Alabama) were weighed, mixed, and dissolved in chloroform at a ratio of DPPC/DOPG 80:20 by weight, and a final lipid concentration of 10 mg/mL. Amyloid-β 1-40 (rPeptide, Bogart, Georgia) was pretreated according to a procedure reported earlier[28,29] by solvation of synthetic peptide with sodium hydroxide followed by lyophilization so as to produce mostly monomeric form of the peptide upon solubilization. The peptide was then dissolved in dimethyl sulfoxide and sonicated for 1 minute. Lipid or BLES surfactant chloroform solution was mixed with amyloid-β solution to obtain solutions with a mixture of 10% amyloid-β by weight. Bovine Lung Extract Surfactant (BLES; BLES Biochemicals) was extracted into chloroform from Goerke's buffer. Then, 0.5 mL BLES in buffer (concentration 27 mg/mL) was mixed with 0.5 mL methanol and 0.5 mL chloroform and the mixture centrifuged for 10 minutes at 100g. The bottom phase was saved, and 0.5 mL chloroform was added to the remaining supernatant. The supernatant was centrifuged again at 100g for 10 minutes, and the bottom phase was again removed and added to the previous bottom phase. The final concentration of the BLES solution was 27 mg/mL. Cholesterol (Avanti Polar Lipids) was added to chloroform solutions of BLES or DPPC-DOPG lipids at 20% by weight.

Langmuir-Blodgett deposition

A freshly cleaved mica slide (ruby, AS™V-2 quality; Asheville-Schoonmaker Mica, Newport News, Virginia) was placed in a dipper arm of the Langmuir-Blodgett trough (LB trough) and lowered into the subphase. We used an LB microtrough from NIMA Technology (Coventry, United Kingdom). Approximately 5–10 μL protein-lipid solutions were deposited on the interface on the LB trough using a 5-μL syringe; the volume of solution added was adjusted to achieve an initial surface pressure of 20 mN/m with the barriers fully open. The lipids were allowed to spread and equilibrate on the interface for 10 minutes. The LB trough barriers were compressed at 10 cm^2/min to collect surface pressure-area isotherms and deposit lipid films on mica at desired compressions. The mica was raised at a rate of 2 mm/min through the interface at constant compression. The mica slide was allowed to air-dry for 10 minutes, than affixed on a glass microscope slide for AFM imaging.

AFM imaging

The lipid films supported on mica slides were imaged in air using a JPK Nanowizard II (JPK Instruments AG, Berlin, Germany) atomic force microscope. Nanoworld AG (Neuchatel, Switzerland) cantilevers with 42 N/m spring constant, and resonance frequency of approximately 250 kHz, were used to image the samples in intermittent contact mode. The topography images of supported lipid films were analyzed using JPK image processing software (JPK Instruments AG). Quantitative analysis of multilayer surface coverage was done using ImageJ software. Images were cropped and converted to a gray scale. The threshold was set to select the first, second, and third multilayers. A particle analysis was done for each multilayer. The number of pixels

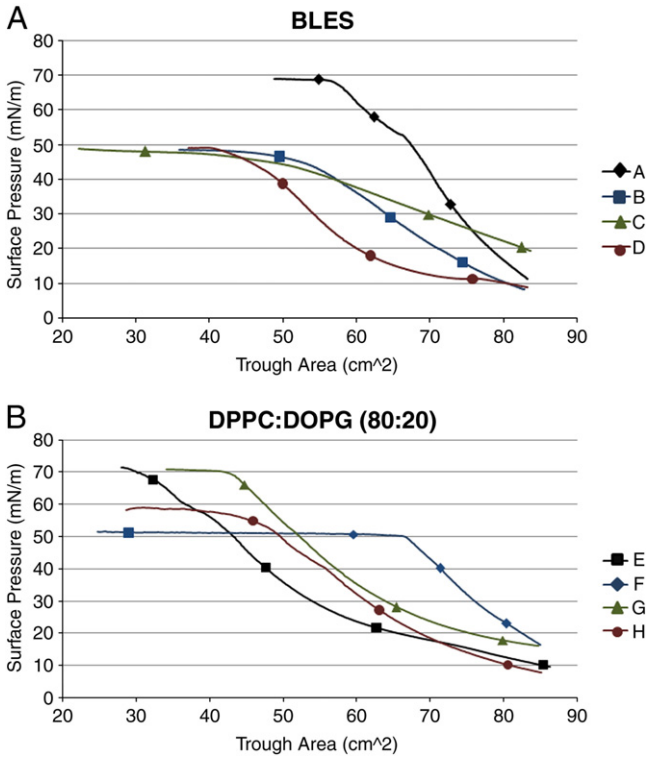

Figure 1. Surface pressure-area isotherms for BLES surfactant and DPPC/DOPG (80:20) compositions. **(A)** BLES surfactant. Curve A, pure BLES; curve B, BLES with 20% cholesterol; curve C, BLES with 10% amyloid-β; curve D, BLES with 20% cholesterol and 10% amyloid-β. **(B)** DPPC/DOPG (80:20). Curve E, pure DPPC-DOPG; curve F, DPPC-DOPG with 20% cholesterol; curve G, DPPC-DOPG with 10% amyloid-β; curve H, DPPC-DOPG with 20% cholesterol and 10% amyloid-β.

displayed was divided by the number of pixels in the image to determine a percentage of surface coverage.

Results

We investigated how addition of amyloid-β 1-40 peptide and addition of cholesterol affect the structure and function of DPPC-DOPG lipid films and BLES surfactant. Using Langmuir-Blodgett monolayer technique, we formed lipid and BLES films at the liquid/air interface and compressed it to mimic the compression of pulmonary surfactant film in the lung.

The LB isotherms, which are plots of compression versus trough area, are presented in Figure 1.

Effect of cholesterol on BLES and DPPC-DOPG mixed-lipid films

First, to investigate the effect of cholesterol, 20% of cholesterol by weight was added to the DPPC-DOPG mixture or to the pure BLES. A Langmuir-Blodgett trough was used to probe surface activity of these films. With no cholesterol, the maximum surface pressure approaches near 70 mN/m for both lipid mixture and BLES (Figure 1, curve A and curve E, respectively), indicating a surface tension near 0 mN/m. The addition of 20% cholesterol to BLES results in a maximum surface pressure of near 50 mN/m (Figure 1, curve B), which is in a good correlation with earlier reported data.[8] Figure 2 shows an AFM topography image of BLES monolayer with (Figure 2, *C*) and without (Figure 2, *A*) 20% of cholesterol, compressed at 45 mN/m and supported on mica by Langmuir-Blodgett deposition. With the absence of cholesterol, the BLES film shows characteristic multilayer patches, as shown in Figure 2 *A*. The schematic of multilayer formation is also shown in Figure 3. Note that discrete multilayers of various shapes with a height of 5 nm and multiples thereof were observed. When 20% cholesterol was present in the film, no multilayers were formed; only small occasional patches or spherical clusters of material were observed (Figure 2, *C*). Surface pressure-area isotherms (Figure 1, *A*, curve B) show a remarkably low compression and plateau at around 48 mN/m, with no further increase in surface pressure, as compared to a plateau at 70 mN/m for pure BLES film (Figure 1, *A*, curve A). This is a result of the cholesterol-inhibiting multilayer formation, which affects both the structure of the film and also the ability of the film to reduce surface tension. These findings correlate well with our previous data.[8,10] Similar to BLES, DPPC-DOPG lipid films also show multilayer formation by AFM (Figure 2, *B*), which correlates with good surface-active properties (Figure 1, *B*, curve E). Figure 2, *D* shows a DPPC-DOPG monolayer with 20% of cholesterol. No multilayer formation was observed in this case, but we observed unusual rodlike patches of lipid material (Figure 2, *D*) that were formed under compression. These rodlike structures have lengths between 0.5 and 3 μm and a height of 8 nm. At the same time the compression of this film failed to reach values higher than 55 mN/m (Figure 1, *B*, curve F).

Effect of addition of amyloid-β to DPPC-DOPG mixed-lipid films and BLES films

Next we added 10% of amyloid-β 1-40 to DPPC/DOPG and BLES with and without addition of cholesterol. When 10% of amyloid-β peptide was added to DPPC-DOPG the number of multilayers formed increased (Figure 2, *F*), compared with Figure 2, *B*. Cross-sectional analysis of the AFM images revealed that these multilayers are multiples of 5 nm high, characteristic of stacks of lipid bilayers. In this case we observed many multilayers of various shapes and heights, similar to that which is present in BLES films. Addition of 10% amyloid-β to BLES showed a decrease in the maximum surface pressure plateau at 48 mN/m, compared to BLES without amyloid-β, shown in Figure 1, *A*, curve C. AFM images (Figure 2, *E*), show that flat peptide-lipid aggregates were found on top of the monolayer. These aggregates reached a height of 30 nm.

Effect of cholesterol and amyloid-β on BLES and DPPC-DOPG mixed-lipid films

BLES with 20% cholesterol and 10% amyloid-β (Figure 2, *G*) showed a return of multilayer formation, compared with cholesterol-laden film without amyloid-β (Figure 2, *C*). Multilayers composed of discrete 5-nm-high bilayers were observed resembling the multilayers in functional BLES. Similar to BLES, DPPC-DOPG (Figure 2, *H*) with 20% cholesterol and 10% amyloid-β also showed a return of multilayers formation. These

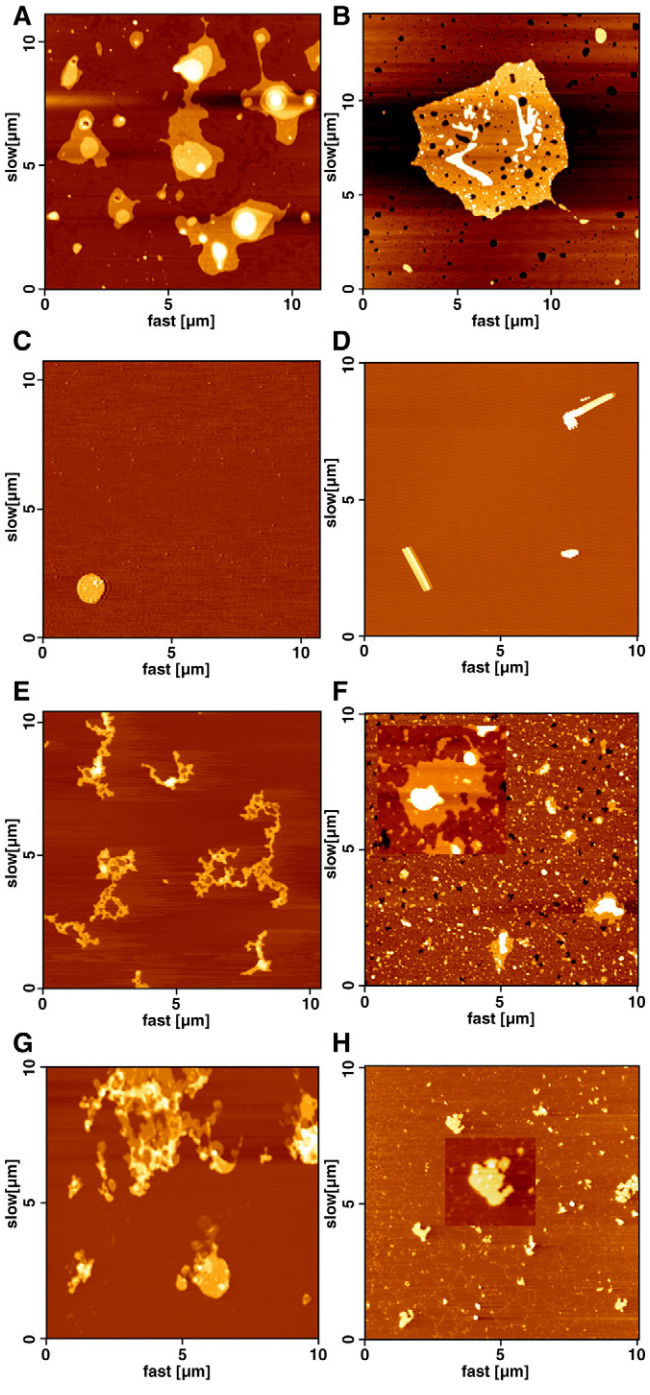

Figure 2. **(A)** AFM topography of BLES-supported film with no cholesterol, compression 50 mN/m, imaged in air. **(B)** AFM topography of DPPC-DOPG film with no cholesterol, compression 45 mN/m, imaged in air.**(C)** AFM topography of BLES film with 20% cholesterol, compression 45 mN/m, imaged in air. **(D)** AFM topography of DPPC-DOPG film with 20% cholesterol, compression 45 mN/m, imaged in air. **(E)** AFM topography of BLES film with 10% amyloid-β added, compression 50 mN/m, imaged in air. **(F)** AFM topography of DPPC-DOPG film with 10% amyloid-β, compression 50 mN/m, imaged in air; inset, high-resolution image of the multilayer. **(G)** AFM topography of BLES with 10% amyloid-β and 20% cholesterol, compression 48 mN/m, imaged in air. **(H)** AFM topography of DPPC-DOPG with 10% amyloid-β and 20% cholesterol, compression 46 mN/m, imaged in air; inset, high-resolution image of the multilayer.

formations seem to have a maximum height of 10 nm, with 5-nm discrete layers. However, these multilayers are smaller than those found in pure DPPC-DOPG mixtures without peptide or cholesterol.

Discussion

We found that for all investigated films, BLES, or DPPC-DOPG, high concentrations of cholesterol impairs surface tension-reducing properties, which are required for proper function of pulmonary surfactant. In surface pressure-area isotherms, we observe a plateau at 48–52 mN/m, with no further increase in surface pressure (Figure 1). We proposed earlier the mechanism by which cholesterol inhibits multilayer formation in BLES,[8,10] probably causing excess material to drop into the liquid subphase as opposed to forming multilayers.[8] The multilayer formation for functional BLES surfactant corresponds to the high surface activity of the film.[8,10] Figure 2, *A* shows a typical BLES multilayer formation. Our data are in good agreement with previously reported data,[8,10] showing that addition of cholesterol to BLES resulted in the abolishment of surface activity of BLES (Figure 2, *C*). In addition, we showed that, similar to BLES, excess cholesterol reduces surface activity and multilayer formation also in DPPC-DOPG lipid mixed films.

When amyloid-β peptide was added to BLES and DPPC-DOPG lipid films, the surface-active properties and film structure were affected. For DPPC-DOPG, both 1% (data not shown) and 10% (Figure 1, *B*, curve F) concentrations of amyloid-β resulted to a high compression (maximum surface pressure plateau for BLES and DPPC-DOPG mixtures of approximately 70 mN/m). This corresponds to the good surface-active properties of functional surfactant. The presence of amyloid-β in DPPC-DOPG leads to multilayer formation with surface coverage and height comparable to that of pure DPPC-DOPG, but the morphology of the multilayers was occasionally different. Multilayers in 10% amyloid-lipid mixtures tended to be smaller and circular in shape (compare Figure 2 *B* and *F*). Table 1 shows statistics on the multilayer surface coverage. Pure DPPC-DOPG films: 8.6% coverage for the first bilayer and higher, 3.7% for the second bilayer and higher. With addition of amyloid-β the first bilayer surface coverage is ~8%, the second bilayer is 2%, and the third bilayer and higher decrease to 1%. These results indicate that for mixed-lipid films DPPC-DOPG, addition of amyloid-β does not disturb multilayer formations, which correlates with good surface-active properties of these films (Figure 1, *B*, curves E and H).

Addition of 10% amyloid-β to BLES, as opposed to lipid mixed films, showed a decrease in surface activity (Figure 1)—decrease in maximum surface pressure and plateau at 48 mN/m (compared with a maximum surface pressure of 70 mN/m in pure functional BLES). AFM images show unique patterns of flat lipid-peptide aggregates (Figure 2, *E*), resembling multilayers, which were flat and have reduced surface coverage. Surface coverage for one bilayer and more was reduced to 6.28 for BLES with 10% amyloid-β, compared with 16.71% for pure BLES; second bilayer and more to 3.18% as compared with 10.48% for pure BLES,

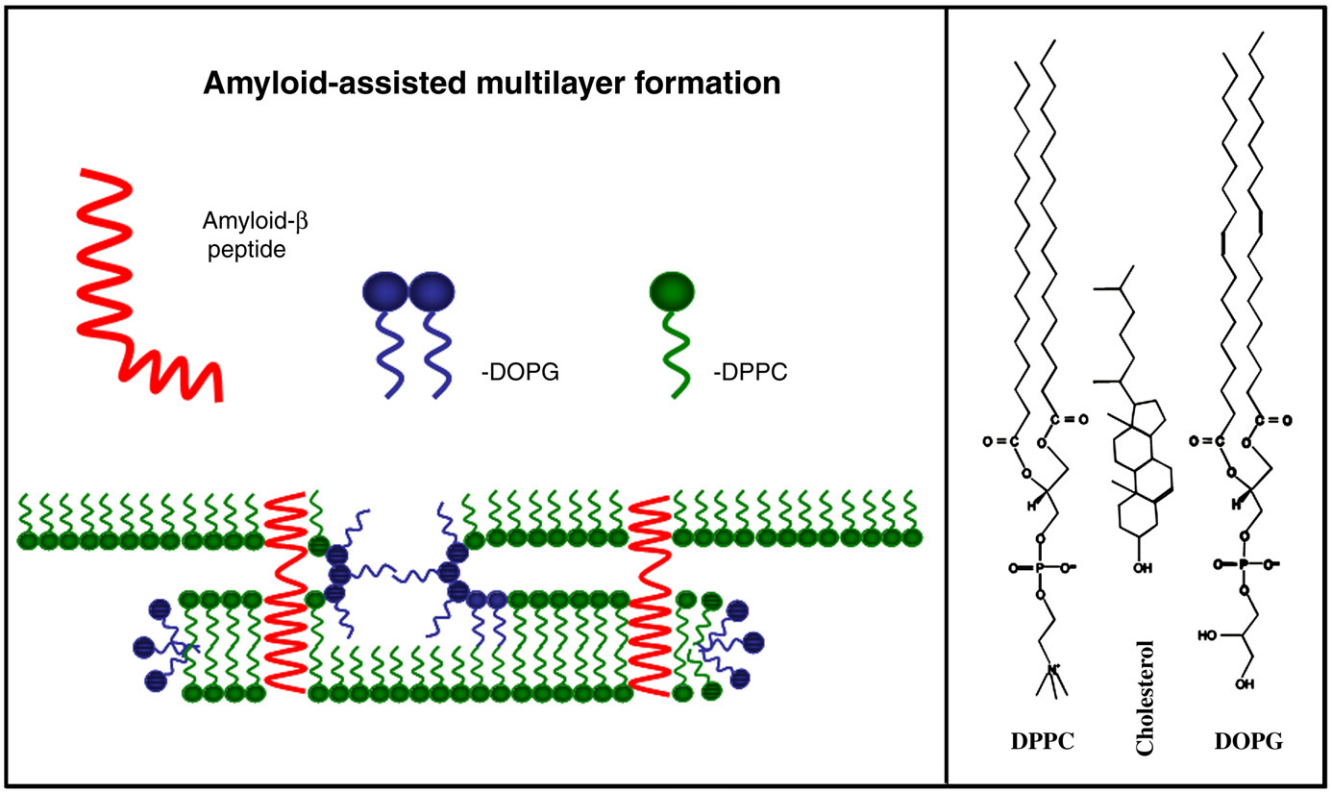

Figure 3. Schematics of multilayer formation assisted by amyloid-β and structures of lipids.

shown in Table 1. From these data we conclude that 10% amyloid-β does not effectively help the multilayer formation characteristic for functional BLES and does not improve surface-active properties of pure BLES.

When both cholesterol and amyloid-β were present in BLES and DPPC-DOPG lipid films, an interesting interplay between these two factors was observed, affecting the structure and surface-active properties of the films. Statistics (Table 1) show that addition of amyloid-β improves surface coverage for cholesterol-laden BLES films (first bilayer and higher 14.05%, second bilayer and higher 3.65%, and third bilayer and higher 1.89%, compared with 0.44%, 0.14, and 0.00 surface coverage for cholesterol-laden BLES films without amyloid-β). BLES contains several proteins whose function is to improve surfactant function, one of them being helical protein SP-C. Cholesterol inhibits surfactant function in BLES, and in mixed-lipid films DPPC-DOPG. However, addition of 10% of amyloid-β 1-40 to both BLES and mixtures of DPPC-DOPG with cholesterol showed return to multilayer formation (Figure 2, *G* and *H*). Surface activity of mixed-film DPPC-DOPG and BLES films was improved upon addition of amyloid-β to cholesterol-laden films. This effect is larger for BLES then for DPPC-DOPG. Although Figure 1 shows a plateau around 50 mN/m, for BLES-cholesterol-amyloid-β, we showed that after a long plateau the film can be compressed to almost 70 mN/m (data not shown) when more material is added. Therefore, 10% amyloid-β 1-40 helps to counteract the dysfunctional effect of cholesterol by assisting the multilayer formation and by improving surface-active properties. Amyloid-β is a two-helix peptide joined with a random coil and can serve as a molecular hinge, similar to SP-C[8] so as to bind and hold lipid multilayers together (Figure 3).

Cholesterol plays an important role in controlling the fluidity, permeability, and mechanical strength of lipid membrane and thus is an important component of lipid rafts.[30-32] Incorporation of cholesterol into lipid bilayers broadens and reduces the enthalpy of phase transitions.[32] Depending on the phase of the lipid, cholesterol decreases (or increases) the cross-sectional area of the phospholipid molecule, as well as increases (or decreases) the thickness of the phospholipid bilayer.[32,33] Importantly, phase separation of phospholipids monolayers in the presence of cholesterol has been visualized by AFM,[34] which showed that lipid monolayer in the presence of cholesterol is composed of domains, related to different phases. The film becomes smooth at high concentrations of cholesterol, where the phase separation becomes invisible. On a molecular level, cholesterol-induced domains have been shown by molecular dynamics simulations.[35] We recently showed that cholesterol induces characteristic electrostatic domains in BLES monolayer, thus changing the electrostatic interactions between lipids and influencing characteristic surface potential distribution in BLES films.[36,37] Research by Ji et al[38] showed that there is a stronger interaction between amyloid-β and cholesterol than between amyloid-β and lipids. It has been shown also that cholesterol induced strong interaction between cholesterol–polyethylene glycol micelles and amyloid-β 1-42.[39] Considering this we postulate that binding of amyloid-β and cholesterol occurs in our BLES and mixed-lipid films, which prevents the cholesterol from saturating the monolayer. When cholesterol saturation of the monolayer is

Table 1
Multilayer surface coverage statistics

	BLES (%)	DPPC/DOPG (%)
Pure film		
1 bilayer or above	16.71	8.60
2 bilayer or above	10.48	3.70
3 bilayer or above	4.35	2.27
+20% Cholesterol		
1 bilayer or above	0.44	1.18
2 bilayer or above	0.14	0.02
3 bilayer or above	0.00	0.00
+10% Amyloid-β		
1 bilayer or above	6.28	7.95
2 bilayer or above	3.18	2.08
3 bilayer or above	1.32	0.97
+20% Cholesterol, 10% amyloid-β		
1 bilayer or above	14.05	3.53
2 bilayer or above	3.65	0.78
3 bilayer or above	1.89	0.05

Quantitative analysis of multilayer surface coverage was completed using ImageJ software. Images were cropped and converted to a gray scale. The threshold was set to select the first, second, and third multilayers. A particle analysis was done for each multilayer. The number of pixels displayed was divided by the number of pixels in the image to determine a percentage of surface coverage.

decreased, the phase separation induced by cholesterol is also decreased, and thus the monolayer becomes more resilient to the cholesterol-induced inhibition of surfactant function. We showed earlier that adhesion properties of the monolayer are strongly inhibited due to the presence of cholesterol, which may prevent an effective multilayer formation.[40]

In summary, we have investigated the effects of addition of cholesterol and amyloid-β 1-40 to BLES surfactant and lipid films composed of DPPC-DOPG. We found that cholesterol impairs surfactant function and decreases the characteristic multilayer formation in both animal extract and lipid mixed films. Surprisingly, the addition of amyloid-β peptide to these surfactants with high concentrations of cholesterol helps to restore multilayer formation in both BLES and DPPC-DOPG mixtures. Therefore amyloid-β 1-40 peptide in the presence of cholesterol excess shows a positive effect on surfactant structure and function, counteracting surfactant failure induced by cholesterol. Despite its negative association in amyloidoses pathogenesis, the positive effect of amyloid-β peptide shown here may serve as an important consideration in the development of artificial surfactant formulations.

Acknowledgments

The authors are thankful to BLES Biochemicals, Inc. for their kind donation of BLES surfactant, as well as JPK Instruments and NIMA Technology Ltd. for their help and outstanding technical support.

References

1. Scarpelli EM, Clutario BC, Taylor FA. Preliminary identification of the lung surfactant system. J Appl Physiol 1967;23:880-6.
2. Holm B, Enhorning G, Notter RH. A biophysical mechanism by which plasma proteins inhibit lung surfactant activity. Chem Phys Lipids 1988; 49:49-55.
3. Floros J, Phelps DS, Pison U, Spragg R. Pulmonary surfactant—update on function, molecular biology and clinical implications. Respir Med Rev 2005;1:77-84.
4. Clements J. Surface tension of lung extracts. Proc Soc Exp Biol Med 1957;95:170-2.
5. Johansson J, Curstedt T. Molecular structures and interactions of pulmonary surfactant components. Eur J Biochem 1997;244:675-93.
6. Crewels LA, van Golde LM, Haagsman HP. The pulmonary surfactant system: biochemical and clinical aspects. Lung 1997;175:1-39.
7. Poulain FR, Clements JA. Pulmonary surfactant therapy. West J Med 1995;162:43-50.
8. Leonenko Z, Gill S, Baoukina S, Monticelli L, Doehner J, Gunasekara L, et al. An elevated level of cholesterol impairs self assembly of pulmonary surfactant into a functional film. Biophys J 2007;93:674-83.
9. Amrein M, von Nahmen A, Sieber M. A scanning force-and fluorescence light microscopy study of the structure and function of a model pulmonary surfactant. Eur Biophys J 1997;26:349-57.
10. Gunasakara L, Schurch S, Schoel M, Kaushik N, Leonenko Z, Haufs M, et al. Pulmonary surfactant function is abolished by an elevated proportion of cholesterol. Biochim Biophys Acta 2005;1737:27-35.
11. Johannsson J. Structure and properties of surfactant protein C. Biochim Biophys Acta 1998;1408:161-72.
12. Li D. The model of the action mechanism of Sp-C in the lung surfactant monolayers. Coll Surf 2007;57:27-8.
13. Nakorn P, Meyer MC, Flach CR, Mendelsohn R, Galla HJ. Surfactant protein C and lung function: new insights into the role of alpha-helical length and palmitoylation. Eur Biophys J 2007;36:477-89.
14. Johannsson J. Amyloid fibrils. FEBS J 2005;272:5941.
15. Gustaffson M. Amyloid fibril formation by pulmonary surfactant protein C. FEBS Lett 1999;464:138-42.
16. Dobson CW. The structural basis of protein folding and its links with human disease. Philos Trans R Soc Lond B Biol Sci 2001;356:133-45.
17. Nelson R, Eisenberg D. Recent atomic models of amyloid fibril structure. Curr Opin Struct Bio 2006;16:260-5.
18. Robertson E, Mucke L. 100 years and counting: prospects for defeating Alzheimer's disease. Science 2006;314:781-5.
19. Kallberg Y, Gustafsson M, Persson B, Thyberg J, Johansson J. Prediction of amyloid fibril-forming proteins. J Biol Chem 2000;276:12945-50.
20. Rauk A. The chemistry of Alzheimer's disease. Chem Soc Rev 2009;38: 2698-715.
21. Engle WA. Surfactant-replacement therapy for respiratory distress in the preterm and term neonate. Pediatrics 2008;121:419-32.
22. Tanaka Y, Takei T, Aiba T, Masuda K, Kiuchi A, Fujiwara T. Development of synthetic lung surfactants. J Lipid Res 1986;27:475-85.
23. Cai P, Flach C, Mendelsohn R. An infrared reflection-absorption spectroscopy study of the secondary structure in (KL4)4K, a therapeutic agent for respiratory distress syndrome, in aqueous monolayers with phospholipids. Biochemistry 2003;42:9446-52.
24. Nakahara H, Lee S, Sugihara G, Chang CH, Shibata O. Langmuir monolayer of artificial pulmonary surfactant mixtures with an amphiphilic peptide at the air/water interface: comparison of new preparations with surfacten (Surfactant TA). Langmuir 2008;24:3370-9.
25. Gustafsson M, Palmblad M, Curstedt T, Johansson J, Schürch S. Palmitoylation of a pulmonary surfactant protein C analogue affects the surface associated lipid reservoir and film stability. Biochim Biophys Acta 2000;1466:169-78.
26. Krol S, Ross M, Sieber M, Kunneke S, Galla HJ, Janshoff A. Formation of three-dimensional protein-lipid aggregates in monolayer films induced by surfactant protein B. Biophys J 2000;79:904-18.
27. Grigoriev D, Kragel J, Akentiev A, Noskov B, Miller R, Pison U. Relation between rheological properties and structural changes in monolayers of model lung surfactant under compression. Biophys Chem 2003;104:633-42.

28. Fezoui Y, Hartley D, Harper J, Khurana R, Walsh D, Condron M, et al. An improved method of preparing the amyloid-β protein for fibrillogenesis and neurotoxicity experiments. Amyloid:. Int J Exp Clin Invest 2000;7:166-78.
29. Choucair A, Chakrapani M, Chakravarthy B, Katsaras J, Johnston LJ. Preferential accumulation of Abeta(1-42) on gel phase domains of lipid bilayers: an AFM and fluorescence study. Biochim Biophys Acta 2007; 1768:146-54.
30. Pike LJ. Rafts defined: a report on the Keystone Symposium on Lipid Rafts and Cell Function. J Lipid Res 2006;47:1597-8.
31. Lingwood D, Simons K. Lipid rafts as a membrane-organizing principle. Science 2010;327:46-50.
32. Pike LJ. The challenge of lipid rafts. J Lipid Res 2009;50(Suppl):S323-8.
33. Kim YH, Tero R, Takizawa U, Urisu T. Characterization of dipalmitoylphosphatidylcholine/cholesterol Langmuir-Blodgett monolayers investigated by atomic force microscopy and Fourier transform infrared spectroscopy. Jpn J Appl Phys I Reg Papers 2004;43:3860-4.
34. Yuan C, Johnston LJ. Phase evolution in cholesterol/DPPC monolayers: atomic force microscopy and near field scanning optical microscopy studies. J Microsc 2002;205:136-46.
35. Murtola T, Karttunen M, Vattulainen I. Systematic coarse graining from structure using internal states: application to phospholipid/cholesterol bilayer. J Chem Phys 2009;055101:131.
36. Finot E, Leonenko Y, Moores B, Eng LM, Amrein M, Leonenko Z. Effect of cholesterol on electrostatics in lipid-protein films of a lung surfactant. Langmuir 2010;26:1929-35.
37. Hane F, Moores B, Amrein M, Leonenko Z. Effect of SP-C on surface potential distribution in pulmonary surfactant: atomic force microscopy and Kelvin-probe force microscopy study. Ultramicroscopy 2009;109: 968-73.
38. Ji SR, Wu Y, Sui SF. Study of β-amyloid peptide (Aβ40) insertion into phospholipid membranes using monolayer technique. Biochemistry (Mosc) 2002;67:1283-8.
39. Kucerka N, Pencer J, Nieh MP, Katsaras J. Influence of cholesterol on the bilayer properties of monounsaturated phosphatidylcholine unilamellar vesicles. Eur Phys J E 2007;23:247-54.
40. Leonenko Z, Finot E, Vassiliev V, Amrein M. The structure and physical properties of BLES surfactant films addressed by atomic force microscopy and force measurements. Ultramicroscopy 2006;106: 687-94.